

1 CAMELS-DE: hydro-meteorological time series and attributes for 2 1582 catchments in Germany

3 Ralf Loritz*¹, Alexander Dolich*¹, Eduardo Acuña Espinoza^{1,A}, Pia Ebeling^{2,A}, Björn Guse^{3,4,A}, Jonas
4 Götte^{5,6,7,A}, Sibylle K. Hassler⁸, Corina Hauffe^{9,A}, Ingo Heidebüchel^{2,10,A}, Jens Kiesel^{3,11,A}, Mirko
5 Mälicke^{1,A}, Hannes Müller-Thomy^{12,A}, Michael Stölzle^{13,A}, Larisa Tarasova^{14,A}

6

7 *equal contribution, A alphabetic order

8 ¹Karlsruhe Institute of Technology (KIT), Institute for Water and Environment, Karlsruhe, Germany

9 ²Helmholtz Centre for Environmental Research - UFZ, Department Hydrogeology, Leipzig, Germany

10 ³Kiel University, Hydrology and Water Resources Management, Kiel, Germany

11 ⁴German Research Centre for Geosciences - GFZ Potsdam, Section Hydrology, Potsdam, Germany

12 ⁵WSL Institute for Snow and Avalanche Research SLF, Davos Dorf, Switzerland

13 ⁶Climate Change, Extremes and Natural Hazards in Alpine Regions Research Center CERC, Davos Dorf

14 ⁷Institute for Atmospheric and Climate Science, ETH Zurich, Zurich, Switzerland

15 ⁸Karlsruhe Institute of Technology (KIT), Institute of Meteorology and Climate Research - Atmospheric Trace Gases and
16 Remote Sensing (IMK-ASF), Karlsruhe, Germany

17 ⁹University of Technology Dresden (TUD), Institute of Hydrology and Meteorology, Dresden, Germany

18 ¹⁰Bayreuth Centre of Ecology and Environmental Research, University of Bayreuth, Bayreuth, Germany

19 ¹¹Stone Environmental, 535 Stone Cutters Way, 05602 Montpelier (VT), USA

20 ¹²Technische Universität Braunschweig, Leichtweiß-Institute for Hydraulic Engineering and Water Resources, Division of
21 Hydrology and River Basin Management, Braunschweig, Germany

22 ¹³Chair of Hydrology, University of Freiburg, Freiburg, Germany, now at: LUBW Landesanstalt für Umwelt (State Agency
23 for Environment), Karlsruhe, Germany

24 ¹⁴Helmholtz Centre for Environmental Research - UFZ, Department Catchment Hydrology, Germany

25

26 *Correspondence to:* Ralf Loritz (Ralf.Loritz@kit.edu) and Alexander Dolich (Alexander.Dolich@kit.edu)

27 **Abstract.** Comprehensive large sample hydrological datasets, particularly the CAMELS datasets (Catchment Attributes and
28 Meteorology for Large-sample Studies), have advanced hydrological research and education in recent years. These datasets
29 integrate extensive hydro-meteorological observations with landscape features, such as geology and land use, across
30 numerous catchments within a national framework. They provide harmonised large sample data for various purposes, such as
31 assessing the impacts of climate change or testing hydrological models on a large number of catchments. Furthermore, these

32 datasets are essential for the rapid progress of data-driven models in hydrology in recent years. Despite Germany's extensive
33 hydro-meteorological measurement infrastructure, it has lacked a consistent, nationwide hydrological dataset, largely due to
34 its decentralised management across different federal states. This fragmentation has hindered cross-state studies and made
35 the preparation of hydrological data labour-intensive. The introduction of CAMELS-DE represents a step forward in
36 bridging this gap. CAMELS-DE includes 1582 streamflow gauges with hydro-meteorological time series data covering up to
37 70 years (median length of 46 years and a minimum length of 10 years), from January 1951 to December 2020. It includes
38 consistent catchment boundaries with areas ranging from 5 to 15,000 km² along with detailed catchment attributes covering
39 soil, land cover, hydrogeologic properties and data about human influences. Furthermore, it includes a regionally trained
40 Long-Short Term Memory (LSTM) network and a locally trained HBV (Hydrologiska Byråns Vattenbalansavdelning) model
41 that were used as quality control and that can be used to fill gaps in discharge data or act as baseline models for the
42 development and testing of new hydrological models. Given the large number of catchments, including numerous relatively
43 small ones (636 catchments < 100 km²), and the time series length of up to 70 years (166 catchments with 70 years of
44 discharge data), CAMELS-DE is one of the most comprehensive national CAMELS datasets available and offers new
45 opportunities for research, particularly in studying long-term trends, runoff formation in small catchments and in analysing
46 catchments with strong human influences. This manuscript describes CAMELS-DE version 1.0, which is available at
47 <https://doi.org/10.5281/zenodo.13837553> (Dolich et al., 2024).

48 **1 Introduction**

49 The CAMELS (Catchment Attributes and MEteorology for Large-sample Studies) datasets have become a cornerstone
50 within the hydrological community for their comprehensive and consistent integration of hydro- and meteorological data
51 across entire countries, including the USA, UK, Australia, Brazil, Chile, and others (e.g. Addor et al., 2017, Coxon et al.,
52 2020). These datasets combine catchment attributes (e.g. land use, geology, and soil properties), hydrological time series
53 (e.g. water level and discharge), and meteorological time series (e.g. precipitation and temperature) for a multitude of
54 catchments typically within a single country. A distinctive feature of CAMELS datasets is their role as a benchmark for
55 hydrological modelling and large sample analysis, enabling the comparison of hydrological models and the validation of
56 water resources management strategies across diverse landscapes and climates (Brunner et al., 2021). Particularly the
57 CAMELS-US dataset has thereby formed the basis for the on-going rise of machine learning methods in hydrology (e.g
58 Kratzert et al., 2019).

59

60 Despite the widespread adoption and utility of CAMELS datasets in research, teaching, and practical applications globally,
61 Germany with its extensive hydro-meteorological measurement network has no comprehensive and harmonised dataset yet.
62 While there are large sample hydrological datasets that cover either parts of Germany (Klingler et al., 2021), only a fraction
63 of the available national hydrological data (Färber et al., 2023), or focus on catchment water quality and thus cover a lower

64 sampling frequency (Ebeling et al., 2022), the absence of a full CAMELS dataset that includes harmonised, daily,
65 high-quality national hydrological and meteorological data together with catchment attributes and catchment boundaries
66 derived from national and international products limits the potential for comprehensive analyses and advancements in
67 hydrological research and practice. The CAMELS-DE data set addresses this gap (Dolich et al., 2024). CAMELS-DE
68 compiles discharge, water levels, catchment attributes, and catchment boundaries together with a suite of meteorological
69 time series and catchment attributes for 1582 catchments across Germany. Furthermore, the dataset includes discharge
70 simulations from two sources: a regionally-trained Long-Short Term Memory (LSTM) network (Hochreiter & Schmidhuber,
71 1997; Hochreiter, 1998), and a locally trained conceptual HBV model (Hydrologiska Byråns Vattenbalansavdelning,
72 Bergström and Forsman, 1973, Seibert, 2005, Feng et al., 2022). These simulations can serve as a benchmark for future
73 hydrological modelling studies in Germany or help fill data gaps in hydrological time series. Each component of the
74 CAMELS-DE processing pipeline is fully containerized (see section 7), which solves code dependency issues and generally
75 contributes to the traceability, comprehensiveness, and reproducibility of the generation of CAMELS-DE. This study
76 introduces not only a comprehensive dataset but also a suite of tools designed to generate reproducible hydrological datasets
77 from the provided raw data. In the following sections we provide a comprehensive description of all data contained within
78 CAMELS-DE including (1) its source data, (2) how the time series and attributes were produced, and (3) a discussion of the
79 associated limitations and uncertainties. The structure of this paper (and also the corresponding dataset) closely mirrors that
80 of the CAMELS-UK (Coxon et al., 2020) and CAMELS-CH (Höge et al., 2023) studies, ensuring comparability of the
81 datasets while maintaining distinct elements that are not identical but closely related.

82 **2 Data sources and providers**

83 CAMELS-DE brings together hydrological data, consisting of daily measurements of discharge ($\text{m}^3 \text{s}^{-1}$) and water levels (m),
84 from thirteen German federal state agencies, namely the Landesanstalt für Umwelt Baden-Württemberg (LUBW,
85 Nomenclature of Territorial Units for Statistics (NUTS) Level 1: DE1), Bayerisches Landesamt für Umwelt (LfU-Bayern,
86 DE2), Landesamt für Umwelt Brandenburg (LfU-Brandenburg, DE4), Hessisches Landesamt für Naturschutz, Umwelt und
87 Geologie (HLNUG, DE7), Landesamt für Umwelt, Naturschutz und Geologie Mecklenburg-Vorpommern (LUNG MV,
88 DE8), Niedersächsischer Landesbetrieb für Wasserwirtschaft, Küsten- und Naturschutz, Landesamt für Natur (NLWKN,
89 DE9), Umwelt und Verbraucherschutz Nordrhein-Westfalen (LANUV NRW, DEA), Landesamt für Umwelt Rheinland-Pfalz
90 (LUA-Rheinland Pfalz, DEB), Landesamt für Umwelt- und Arbeitsschutz Saarland (LUA, DEC), Landesamt für Umwelt,
91 Landwirtschaft und Geologie Sachsen (LfULG, DED), Landesamt für Umweltschutz Sachsen-Anhalt (LAU, DEE),
92 Landesamt für Landwirtschaft, Umwelt und ländliche Räume Schleswig-Holstein (LLUR, DEF), and Thüringer Landesamt
93 für Umwelt, Bergbau und Naturschutz (TLUBN, DEG). The only federal states not included are the city-states of Bremen,
94 Hamburg, and Berlin, which together account for less than 0.6 % of Germany's area, ensuring that the CAMELS-DE dataset
95 remains representative for Germany.

97 Meteorological data, specifically precipitation, temperature, relative humidity and radiation, were obtained from the German
98 Weather Service (DWD) from the HYRAS dataset (DWD-HYRAS, 2024). Spatially aggregated catchment attributes were
99 obtained from various sources. From the European Union, we incorporated open-access datasets from Copernicus, the EU's
100 Earth observation program, in particular the Copernicus GLO-30 DEM (Global 30-meter Digital Elevation Model;
101 EU-DEM, 2022) for information about topography and the CORINE Land Cover 2018 dataset (CLC, 2018) for information
102 about land cover. Soil attributes were derived from the global SoilGrids250m dataset (Poggio et al., 2021). Hydrogeological
103 catchment attributes were derived from the “Hydrogeologische Übersichtskarte von Deutschland 1:250.000” (HGM250,
104 2019) provided by the Bundesanstalt für Geowissenschaften und Rohstoffe (BGR) while information about human
105 influences, e.g. dams or weirs, was sourced from Speckhann et al. (2021).

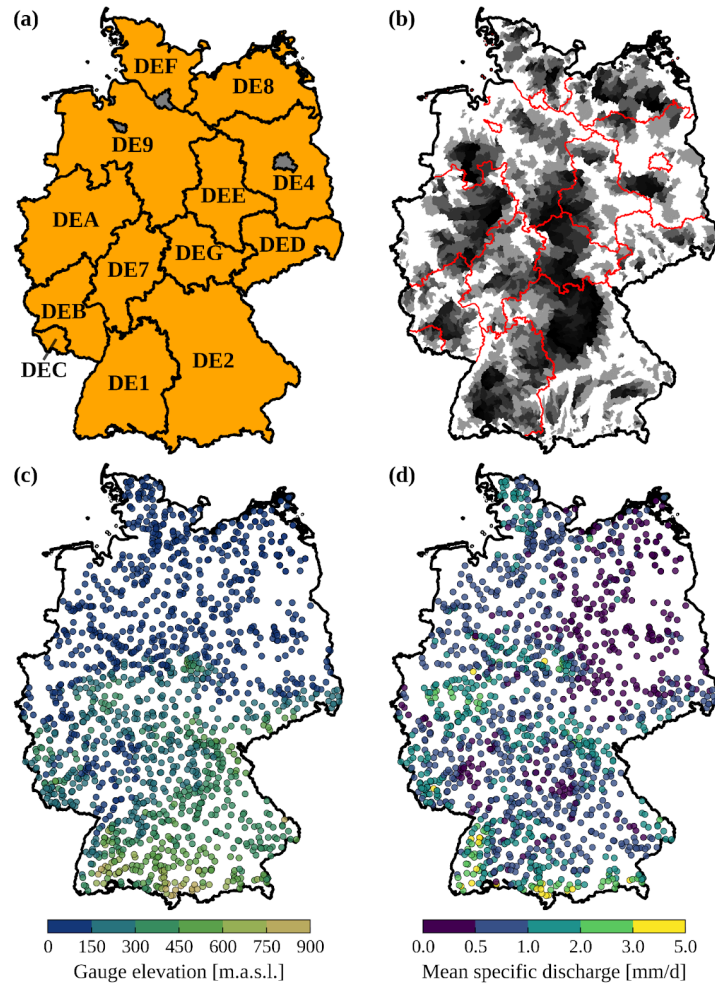
106 3 Catchments

107 For CAMELS-DE, we sourced discharge ($\text{m}^3 \text{s}^{-1}$), water level data (m) and metadata for 2964 gauges and water level stations
108 from the different federal state agencies (see section 2). We created a subset of the data by selecting only measurement
109 stations that contained all required information, such as gauge name, location and catchment area in their metadata ($n = 2700$
110 stations), have at least a total of 10 years of discharge data, which must not necessarily be continuous ($n = 2227$ stations),
111 have a catchment area larger than 5 km^2 and smaller than $15,000 \text{ km}^2$ ($n = 2586$ stations), have a catchment area located
112 entirely within the borders of Germany ($n = 2298$ stations) and where the derived catchment area does not differ more than
113 20 % from the reported value by the federal states ($n = 2164$ stations; see section 3.1). These requirements were established
114 based on the following rationale: A minimum of 10 years of discharge data is necessary to ensure an adequate time series
115 length for hydrological modelling and calculating hydrological signatures. The minimum catchment area of 5 km^2 was
116 chosen to match the $1 \times 1 \text{ km}$ resolution of the precipitation raster product, ensuring that multiple raster cells intersect with
117 the catchment boundary. The upper limit was set because catchments larger than $15,000 \text{ km}^2$ are predominantly influenced
118 by human activities and often extend beyond Germany's borders, necessitating their exclusion. The 20 % discrepancy
119 between derived and reported catchment areas was arbitrarily chosen as an acceptable threshold for mass balance errors. This
120 threshold prevents the inclusion of catchments with significantly inaccurate delineations while avoiding the exclusion of too
121 much data (see Fig. 2b). Catchments partially located outside Germany's borders were excluded to avoid complications with
122 cross-border data, especially given the absence of open, high-quality meteorological data from the DWD beyond Germany's
123 national borders from 1951 to 2020. These criteria resulted in a subset of 1582 gauges for the CAMELS-DE dataset, which
124 provides a reliable representation of hydrological processes in Germany (Fig. 1c, d).

125 3.1 Catchment boundaries

126 Not all state authorities provided official catchment boundaries for their gauging stations, and the methods used by the
127 federal states to derive these boundaries are not uniform and remain unclear. Therefore, we tested two different global
128 catchment datasets, HydroSHEDS (Lehner et al., 2021) and MERIT Hydro (Yamazaki et al., 2019), to derive a consistent set
129 of catchment boundaries across Germany for the CAMELS-DE dataset. For that we compared the catchment areas
130 determined with HydroSHEDS and MERIT Hydro to the catchment areas reported by the state authorities. This comparison
131 was possible because all federal states shared the area of the catchments while not always sharing the actual catchment
132 boundaries. Overall, the comparison revealed that MERIT Hydro has lower errors between the reported and derived
133 catchment areas compared to HydroSHEDS. Among other reasons, this is because MERIT Hydro derives the catchment
134 boundaries directly at the gauge locations provided by the federal states (see section 3.2). The comparison between MERIT
135 Hydro and HydroSHEDS was further supported by extensive manual assessments, involving the visual inspection of
136 numerous catchments to evaluate their shapes and alignments in case the federal state provided the data. Consequently,
137 MERIT Hydro was used for the derivation of catchment boundaries for CAMELS-DE. Note that the derivation of the
138 catchment boundaries is a major source of uncertainty as the meteorological time series and the catchment attributes are
139 dependent on the catchment boundaries. To minimise the uncertainty of the catchment delineation we only included
140 catchments with a deviation of up to 20 percent from the catchment area reported by the federal agencies (Fig. 2b). We report
141 the original catchment area as (area_metadata) and the MERIT-Hydro based area (area) in the table of topographic attributes
142 (Table 2).

143



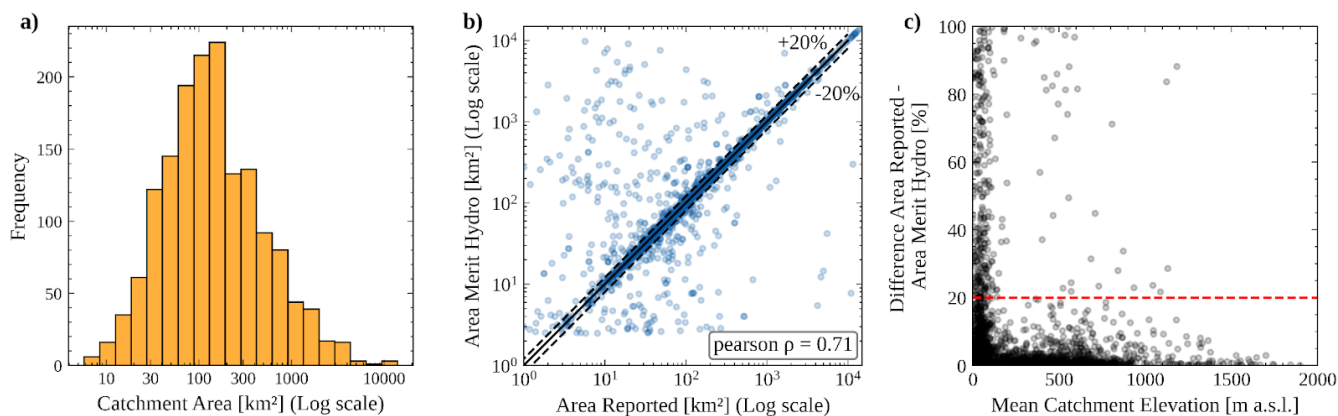
144

145 **Figure 1:** Panel (a) shows the German federal states labelled with their NUTS Level 1 ID as used for the CAMELS-DE gauge IDs. Panel (b) shows all 1582
 146 catchments provided in CAMELS-DE, the geometries of the catchments are shown transparently, so a darker colour means that the geometries of the
 147 catchments in that area overlap; the darker the colour, the higher the density of catchments in that area. Panel (c) and panel (d) show the location of all 1582
 148 gauging stations in CAMELS-DE; in panel (c) the locations are coloured according to the elevation of the gauging station, while in panel (d) the locations
 149 are coloured according to their mean specific discharge value. borders of Germany: © GeoBasis-DE / BKG (VG250, 2023)

150 3.2 Catchment boundaries derived from MERIT Hydro

151 MERIT (Multi-Error-Removed Improved-Terrain) Hydro was released by Yamazaki et al. (2019); providing a global
 152 hydrography dataset based on the MERIT DEM and various maps of water bodies (e.g. Global 3 arc-second Water Body
 153 Map by Yamazaki et al., 2017). It includes information such as flow direction, flow accumulation, adjusted elevations for
 154 hydrological purposes, and the width of river channels. The delineator.py package (Heberger, 2023) was used to delineate
 155 catchment boundaries. The method automatically derives catchment boundaries from the MERIT Hydro dataset based on the
 156 longitude and latitude of a gauging station and snaps the catchment pour point to the closest stream. Fig. 1b shows all
 157 derived CAMELS-DE catchments using MERIT Hydro within the German borders. The median catchment area within

158 CAMELS-DE is 129.1 km² (Fig. 2a). Compared to other CAMELS datasets, CAMELS-DE includes a large number of
 159 relatively small catchments with an area of less than 100 km² (i.e. 636 catchments, CAMELS-GB: 242 catchments,
 160 CAMELS-US: 142). Uncertainties in catchment delineation arise when comparing areas reported by federal states with those
 161 derived from MERIT Hydro, as shown in Fig. 2b, and these discrepancies are not uniformly distributed across Germany.
 162 They tend to be higher in flat lowland regions with minimal topography (Fig. 2c), particularly in the federal states to the
 163 north and east of Germany. Consequently, a large number of catchments are excluded from the CAMELS-DE dataset in the
 164 northern parts of Germany due to mismatches between reported and estimated areas. In the federal states of Brandenburg
 165 (DE4) and Mecklenburg-Western Pomerania (DE8), for example, we received 447 gauging stations, but given the
 166 uncertainty of the delineation in flat areas, only 277 of them showed a deviation of less than 20 percent from the reported
 167 area. In contrast, in the more mountainous state of Baden-Württemberg (DE1), 225 of 241 catchments met this criterion. As
 168 we report both the catchment areas provided by the federal states and those estimated by MERIT Hydro, the differences
 169 between these two measurements can be used to select or exclude catchments where there are significant uncertainties in the
 170 catchment shape and correspondingly in the derived static and dynamic attributes.



172 **Figure. 2:** Panel (a) shows the distribution of CAMELS-DE catchment areas on a logarithmic scale. Panel (b) shows the accuracy of catchment areas
 173 derived using MERIT Hydro compared to the area reported by the federal agencies; the dashed lines indicate ± 20 percent error tolerance that was set for
 174 catchment selection. Panel (c) shows the absolute relative difference between the reported area by the federal states and the MERIT Hydro area against the
 175 mean catchment elevation. The red line marks the threshold of 20 percent allowed difference for the inclusion of a catchment in the CAMELS-DE dataset.

176 4 Time series

177 CAMELS-DE includes three sets of hydro-meteorological daily time series, as detailed in Table 1, covering the period from
 178 January 1, 1951, to December 31, 2020. These datasets are: (A) observed hydrologic time series (e.g., station discharge and
 179 water levels), (B) observed meteorologic time series (e.g., precipitation, temperature, humidity, and radiation), and
 180 simulated hydro-meteorologic time series (e.g., discharge simulated by a LSTM and a HBV model, including estimated
 181 evapotranspiration). Note that we do not include any information on evaporation in the non-simulated time series data, as we
 182 only include observation-based data here. However, a time series of potential evaporation based on the temperature-based

183 Hargreaves methodology is included in the simulated data (see section 6.2 for more details). However, due to the simplicity
184 of the chosen approach, the potential evapotranspiration time series are highly uncertain, and one should exercise caution
185 when using them.

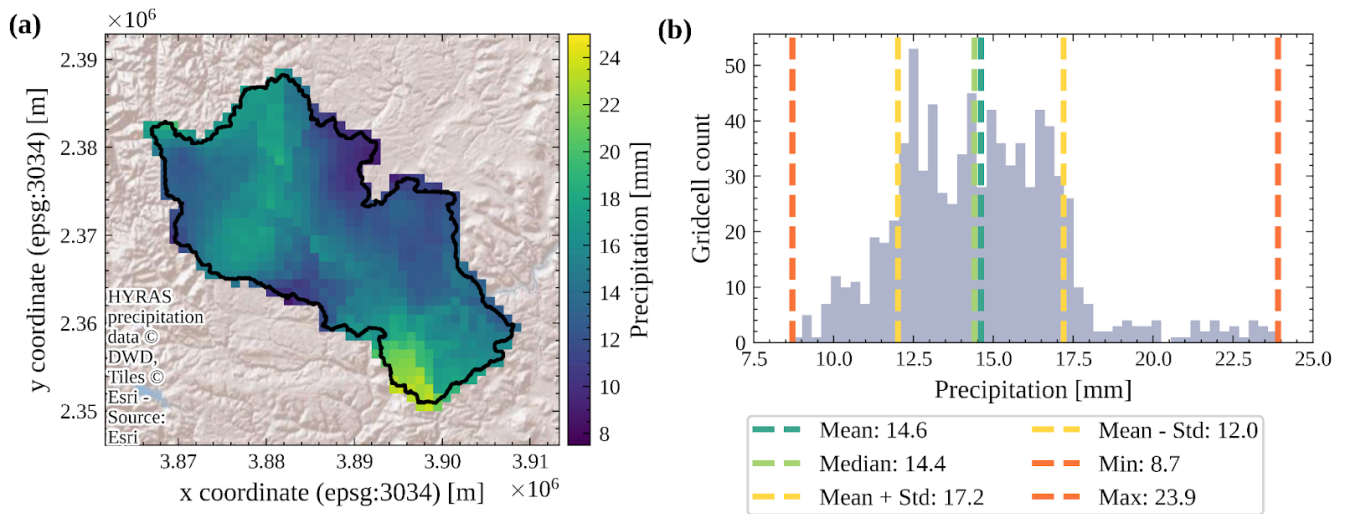
186

187 All meteorological forcing data within CAMELS-DE are sourced from the HYRAS datasets, which are based on the
188 interpolation of meteorological station data (DWD-HYRAS, 2024). This interpolation was conducted by the DWD (see
189 subsection 4.1, 4.2, 4.3). The reliability of these datasets can be compromised by the individual interpolation methods
190 employed (see section 4.1 to 4.3). In addition, inaccuracies in meteorological measurements can introduce uncertainties in
191 the generated grid fields, especially given the extended timescale of 70 years, which may include changes in location and
192 sensor types. Another source of uncertainty is the fact that the number of stations used in the interpolation process varies
193 over time, mirroring changes in the measurement network. For example, the number of stations used for interpolating
194 precipitation data fluctuates, starting at around 4500 in 1951, peaking at approximately 7500 in 2000, and then decreasing to
195 approximately 5000 by 2020. In contrast, the number of stations used for radiation interpolation shows a consistent increase
196 over the years, though the total number remains significantly lower, reaching about 900 stations by 2020. This uncertainty is
197 crucial to consider when comparing data across different years, particularly if the focus is on a single or a few catchments in
198 a certain area. Finally, we use the ‘exact extract’ method, which ensures that raster cells that are only partially covered are
199 treated properly as they are weighted by the proportion of the cell that is covered, i.e. a raster cell that is only 20 % covered
200 by the catchment is only weighted by 20 % when we aggregate to the spatial catchment mean (Fig. 3a illustrates partially
201 covered cells at the catchment boundary). This is particularly important when deriving meteorological data for very small
202 catchment areas. Although this approach also aids in comparing products with different resolutions, it is important to
203 consider that the spatial resolution of the precipitation data, at 1 x 1 km, offers finer detail compared to the 5 x 5 km
204 resolution used for temperature, humidity, and radiation data. This difference is crucial when comparing these datasets within
205 smaller catchments.

206 **4.1 Precipitation**

207 CAMELS-DE utilises precipitation data (mm d^{-1}) with daily resolution, sourced from the HYRAS-DE-PRE dataset v5.0
208 (HYRAS-DE-PRE, 2022). We have calculated daily spatial minimum, mean, median, maximum, and standard deviation of
209 the rainfall field over the catchment for each day. We estimated these statistical measures, rather than just the mean, because
210 this allows us to capture spatial variations and patterns that can be crucial for event characterization or rainfall-runoff
211 modelling, as illustrated in Fig. 3. The HYRAS-DE-PRE dataset v5.0 dataset is produced using the REGNIE interpolation
212 method (Rauhe et al., 2013), which employs daily measured values from meteorological stations to generate an interpolated
213 product on a 1x1 km grid. A detailed description of the interpolation method and the related uncertainties can be found in the
214 official data description (HYRAS-DE-PRE, 2022).

215



216

217 **Figure 3:** Panel (a) shows the catchment boundaries (black line) of the catchment Kirchen-Hausen in Baden-Württemberg overlaid by a clipped daily
 218 precipitation field from the HYRAS dataset on the date 1951-02-20. Panel (b) shows the spatial distribution of rainfall during the same high precipitation
 219 event as (a) over the catchment on 1951-02-20 and the statistical moments (mean, median, standard deviation, minimum and maximum) derived from the
 220 spatial distribution.

221 4.2 Temperature and relative humidity

222 CAMELS-DE employs daily temperature ($^{\circ}\text{C}$) and relative humidity (%), derived from the HYRAS-DE-TAS (daily mean
 223 temperature, HYRAS-DE-TAS, 2022), TASMING (daily minimum temperature, HYRAS-DE-TASMIN, 2022), TASMING
 224 (daily maximum temperature, HYRAS-DE-TASMAX, 2022), and HURS (daily average relative humidity,
 225 HYRAS-DE-HURS, 2022) datasets v5.0, which cover the period from 1951 to 2020 on a 5 km x 5 km grid. This includes the
 226 spatial mean, median, and standard deviation of temperature from HYRAS-DE-TAS, alongside the spatial minimum and
 227 maximum temperatures from TASMING and TASMING, respectively. Additionally, for humidity, we integrate daily minimum,
 228 mean, median, maximum, and standard deviation values across the catchment area. The temperature and humidity data is
 229 based on interpolated station values (Razafimaharo et al., 2020). This interpolation method involves a nonlinear regression at
 230 each time step, aiming to estimate regional vertical temperature profiles across 13 subregions. These subregions are
 231 delineated based on criteria such as weather divides, proximity to the coast, and the extent of north-south variation. A
 232 detailed description of the interpolation method and the related uncertainties can be found in the corresponding data
 233 descriptions (HYRAS-DE-TAS, (2022); HYRAS-DE-TASMIN, (2022); HYRAS-DE-TASMAX, (2022);
 234 HYRAS-DE-HURS, (2022)).

235 4.3 Radiation

236 The CAMELS-DE dataset utilises daily mean global radiation data (in W m^{-2}) derived from the HYRAS-DE-RSDS datasets
 237 v3.0 (HYRAS-DE-RSDS, 2023), that covers a period from 1951 to 2020 with a 5 km x 5 km grid. We have derived daily,

238 spatial minimum, mean, median, maximum, and standard deviation of the radiation field over the catchment for each day.
239 The global radiation (RSDS) dataset integrates station measurement data (including sunshine duration and global radiation),
240 satellite data, and ERA5 data (Muñoz-Sabater et al., 2021). A detailed description of the interpolation method and the related
241 uncertainties can be found in the official data description (HYRAS-DE-RSDS, 2023).

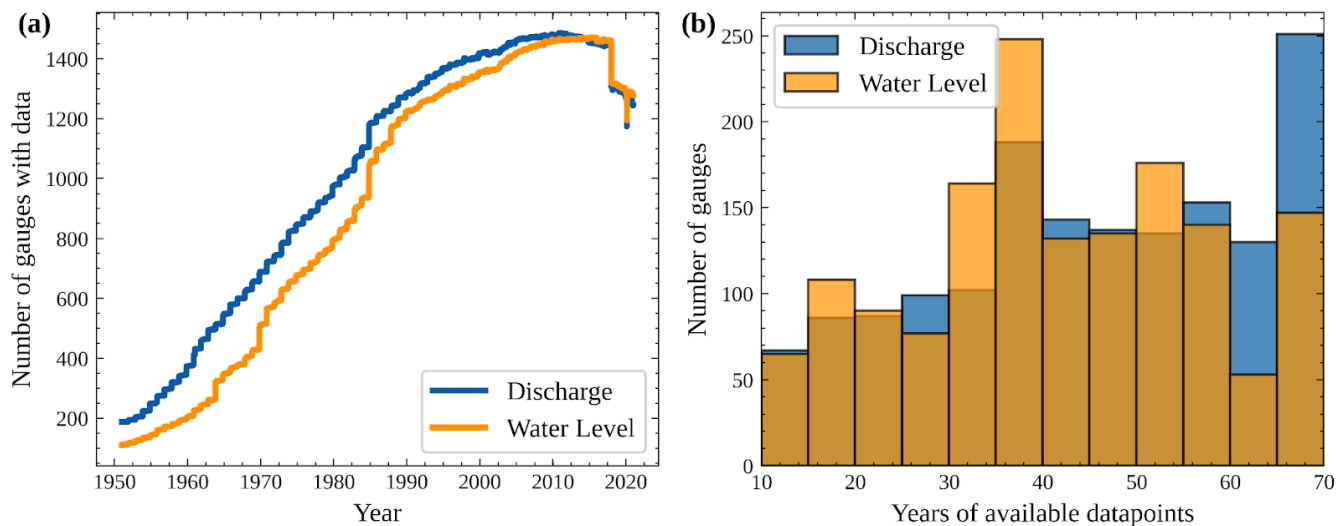
242 **4.4 Discharge and water levels**

243 Observed discharge and water level data were requested from 13 state agencies (see section 2) as time series recorded at the
244 gauging stations (Tab. 1). The number of stations with daily discharge data available per year increases in time from 187 on
245 1 January 1951 to a maximum of 1486 between November 2010 and February 2011 (Fig. 4a). The number of stations with
246 water level data is generally lower, starting at 110 stations on 1 January 1951 and reaching a maximum of 1471 stations
247 between March 2015 and December 2015. The time series span a maximum of 70 years, with each measuring station
248 providing at least 10 years of data between January 1951 and December 2020 (Fig. 4b). These 10 years do not need to be
249 consecutive but typically are. The median time series length of discharge is 46 years, while the median time series length of
250 water level is 40 years. There is a sharp drop-off in Fig. 4a of 137 stations without data from 2017 to 2018 as the provided
251 data from NLWKN (Lower Saxony, DE9) only range until the end of 2017. Another anomaly in Fig. 4a is the drop
252 immediately followed by a rise in the year 2020, which is due to the fact that all measuring stations in Rhineland-Palatinate
253 (DEB) show a gap in the discharge data from 10 February 2020 to 15 February 2020 and in the water level data from 13
254 February 2020 to 15 February 2020. No explanation could be found for this gap. The remaining data after the gap was
255 manually quality controlled by visual inspection of the observed and simulated time series and no reason to exclude this data
256 was found. In total, CAMELS-DE includes 156 stations for which the entire temporal range of 70 years of discharge data is
257 available and for which a maximum of 2 percent of the data is missing in this period. There are 85 stations where this is the
258 case for water level data.

259 **4.5 Discharge and water levels - quality control**

260 The quality control of all discharge and water level data was conducted by the respective federal states (quality controlled
261 data was requested). However, the specific methods employed in this quality control are neither the same across the states,
262 nor are they documented in some cases. Typically, quality control entails that a technical clerk has visually inspected the
263 hydrological time series data. To account for this uncertainty we conducted an additional review of all time series data for
264 high negative values and unrealistically high outliers and replaced such data points with not-a-number (NaN) values. We
265 were conservative in these cases and only deleted values that were clear data errors to not remove potential extreme flood
266 events from the time series. This adjustment was necessary in 8 catchments and is documented in the processing pipeline to
267 assure reproducibility. Please note that negative discharge values are still possible in the CAMELS-DE dataset due to the
268 influence of the tide in the northern part of Germany or due to human influences related to water resources management.
269 Moreover, we assessed the hydro-meteorological time series using both a hydrological model and a data-driven model. This

270 analysis helped us identify catchments with weak correlations between meteorological conditions and hydrological responses
 271 as well as catchments in which the mass balance is far from being closed. All catchments that exhibited a low model
 272 performance of the HBV model were subjected to manual visual inspection, resulting in the removal of 14 catchments (for
 273 more details we refer to section 6).



274
 275 **Figure 4:** Panel (a) shows the number of gauging stations with available discharge (blue) and water level data (orange) in the period from 1951 to 2020,
 276 taking into account data gaps, i.e. the data must actually be available at the respective time. Panel (b) shows a histogram of the years of available data points
 277 for all measuring stations, i.e. the length of the time series minus eventual gaps in the time series.

278
 279 **Table 1:** Catchment-specific hydro-meteorological variables available as daily time series in CAMELS-DE

Time series class	Time series name	Description	Unit	Data source
Hydrologic time series (1 Jan 1951–31 Dec 2020)	discharge_vol	Observed catchment discharge calculated from the water level and gauge geometry	$\text{m}^3 \text{s}^{-1}$	Federal state agencies (see section 2)
	discharge_spec	Observed catchment-specific discharge (converted to millimetres per day using catchment areas described in section 3.1)	mm d^{-1}	
	water_level	Observed daily water level	m	
Meteorologic time series (1 Jan 1951–31 Dec 2020)	precipitation_mean, precipitation_median, precipitation_min, precipitation_max, precipitation_stdev	Observed interpolated spatial mean, median, minimum, maximum and standard deviation of the daily precipitation (original resolution $1 \times 1 \text{ km}^2$)	mm d^{-1}	German Weather Service HYRAS (DWD-HYRAS, 2024)
	temperature_min	Observed interpolated spatial mean daily minimum temperatures (original resolution $5 \times 5 \text{ km}^2$)	$^{\circ}\text{C}$	
	temperature_mean	Observed interpolated spatial mean daily mean	$^{\circ}\text{C}$	

		temperatures (original resolution 5x5 km ²)			
	temperature_max	Observed interpolated spatial mean daily maximum temperatures (original resolution 5x5 km ²)	°C		
	humidity_mean, humidity_median, humidity_min, humidity_max, humidity_stdev	Observed interpolated spatial mean, median, minimum, maximum and standard deviation of the daily humidity (original resolution 5x5 km ²)	%		
	radiation_global_mean, radiation_global_median, radiation_global_min, radiation_global_max, radiation_global_stdev	Observed interpolated spatial mean, median, minimum, maximum and standard deviation of the global radiation (original resolution 5x5 km ²)	W m ²		
Simulated hydrologic time series (1 Jan 1951–31 Dec 2020)	pet_hargreaves	Daily mean of potential evapotranspiration calculated using the Hargreaves equation	mm d ⁻¹	Regional LSTM model, HBV model and Hargreaves equation for potential evapotranspiration (see section 6, https://github.com/KIT-HYD/Hy2DL/tree/v1.1 , last access: 24 July 2024)	
	discharge_vol_obs	Observed volumetric discharge	m ³ s ⁻¹		
	discharge_spec_obs	Observed catchment-specific discharge	mm d ⁻¹		
	discharge_vol_sim_lstm	Volumetric discharge calculated from discharge_spec_sim_lstm and the catchment area	m ³ s ⁻¹		
	discharge_spec_sim_lstm	Catchment-specific discharge simulated with the LSTM (see section 6)	mm d ⁻¹		
	discharge_vol_sim_hbv	Volumetric discharge calculated from discharge_spec_sim_hbv and the catchment area	m ³ s ⁻¹		
	discharge_spec_sim_hbv	Catchment-specific discharge simulated with the HBV model (see section 6)	mm d ⁻¹		
	simulation_period (training, validation, testing)	Flag indicating the simulation period in which the daily value is contained (training, validation, testing)	–		

280 5 Catchment attributes

281 In addition to the daily time series of hydro-meteorological variables available in CAMELS-DE, the dataset also includes a
282 series of static catchment attributes which are considered time-invariant and include information about topography (section
283 5.1), hydroclimatic signatures (section 5.2) and catchment attributes covering land-cover (section 5.3), soil (section 5.4),
284 hydrogeology (section 5.5) and human influences (section 5.6).

285 5.1 Location and topography

286 For CAMELS-DE, we developed a system of catchment IDs, since the official IDs used by the federal states are inconsistent
287 beyond federal state boundaries. However, the official provider IDs are contained in the topographic attributes of the dataset

288 (Tab. 2). The gauge IDs in CAMELS-DE are based on the NUTS classification, which divides the EU territory hierarchically
289 according to administrative boundaries. In Germany, the first hierarchical level NUTS 1 provides a code for each federal
290 state (e.g. DE7 for Hessen, DED for Saxony; Fig. 1b). We assign an ID code to each gauge as follows. The ID of each gauge
291 starts with the NUTS 1 code of the corresponding federal state. For each federal state the gauges are coded in arbitrary order
292 starting from 10000 for the first gauge and adding a step of 10 for each following gauge (e.g. DE710000 for the first station
293 in Hessen, DE710010 for the second station, DE710020 for the third station, etc.). This system ensures consistency of the
294 gauge IDs in Germany, and additionally provides the information about the federal state of each gauge. Topographic
295 attributes such as the location (coordinate systems WGS84 and ETRS89), gauge elevation (m) and catchment area (km²)
296 were provided by the federal agencies, the area of the MERIT Hydro catchment is also provided. Additionally we derived the
297 gauge point elevation (m) and basic statistical variables (min, mean, median, 5th and 95th percentile, max) of the catchment
298 elevation (m) from the GLO-30 DEM. CAMELS-DE additionally provides the location of all gauging stations and catchment
299 boundaries as a shape file and a geopackage file.

300 5.2 Climate and hydrology

301 For the CAMELS-DE dataset, we calculated long-term climatic and hydrological signatures in line with the attributes found
302 in CAMELS-CH (covering the period between 1981–2020) and CAMELS-UK (covering the period between 1970–2015)
303 with the difference that we cover the period from 1951–2021 (see Tab. 2). Both types of attributes are calculated based solely
304 on complete hydrological years with respect to the discharge (1 October to 30 September of the following year; again inline
305 with the definition of a hydrological year chosen in CAMELS-UK and CAMELS-CH), with a maximum tolerance of 5 %
306 missing values per hydrological year, ensuring robustness in the data used for analysis. If a specific catchment has discharge
307 data for only a limited number of hydrologic years, we calculate the climatic and hydrological indices for those same years to
308 maintain consistency across all CAMELS datasets and across the climatic and hydrological attributes.

309

310 For each catchment, the hydrologic attributes include values for the mean specific discharge (mm d⁻¹), the runoff ratio, the
311 start and end dates of available discharge data, the percentage of days on which discharge data is available (%), the slope of
312 the flow duration curve between the log-transformed 33rd and 66th percentiles, the number of days after which the
313 cumulative discharge since 1 October reaches half of the annual discharge (d), the 5th and 95th quantile of specific discharge
314 (mm d⁻¹) and the frequency of high flow, low flow and zero flow days (d yr⁻¹) together with the average duration of high-flow
315 and low-flow events (d). The climatic attributes are calculated on the basis of the HYRAS meteorological data for each
316 catchment and include mean daily precipitation (mm d⁻¹), the seasonality of precipitation, the fraction of precipitation falling
317 as snow, the frequency of high and low precipitation days (d yr⁻¹), the average duration of high precipitation events and dry
318 periods (d) as well as the season during which most high and low precipitation days occur. The code to estimate the
319 signatures in CAMELS-DE is based on the codes used to derive the signatures for CAMELS-US
320 (<https://github.com/naddor/camels>, last access: 19 July 2024), CAMELS-UK and CAMELS-CH to assure compatibility.

321 **5.3 Land cover**

322 Land cover in CAMELS-DE is derived from the Corine Land Cover dataset (CLC, 2018) which provides consistent and
323 thematically detailed information on land cover across Europe. The dataset was produced within the frame of the Copernicus
324 Land Monitoring Service referring to land cover / land use status of the year 2018 and is based on the classification of
325 satellite images (other major releases have been published in the years 1990, 2000, 2006, 2012). The CLC dataset from 2018
326 has a spatial resolution of 100 m for raster data. This ensures detailed and consistent land cover information across Europe.
327 CAMELS-DE includes land cover percentages per catchment of the first hierarchical land cover level: artificial surfaces,
328 agricultural areas, forests and semi-natural areas, wetlands and water bodies. The decision to not mix the hierarchical land
329 cover levels ensures that uncertainties in classification due to varying levels of detail are minimised. Catchment shapes and
330 codes to derive land cover classes of lower order or from different releases of CLC in a consistent manner with
331 CAMELS-DE are delivered with the dataset (Dolich, 2024).

332 **5.4 Soil**

333 Soil attributes for CAMELS-DE are derived from the SoilGrids250m dataset (Poggio et al., 2021), which maps the spatial
334 distribution of soil properties globally at six standard depths. The SoilGrids dataset is generated by training a machine
335 learning model on approximately 240,000 locations worldwide, using over 400 global environmental covariates that describe
336 vegetation, terrain morphology, climate, geology, and hydrology. For CAMELS-DE, we derived the mean values of the soil
337 bulk density, soil organic carbon, volumetric percentage of coarse fragments and proportions of clay, silt and sand for each
338 catchment. The resulting variables are aggregated from the six SoilGrid depths to the depths 0-30 cm, 30-100 cm and
339 100-200 cm by calculating a weighted mean. The accuracy of soil property models, as described by Poggio et al. (2021), is
340 limited by the availability and quality of input data and the assumptions in the modelling process. For instance, discrepancies
341 in how soil data are collected, analysed, and reported by different entities challenge efforts toward data standardisation and
342 harmonisation. However, the relatively high number of observations in Germany reduces this uncertainty to a certain extent.
343 Furthermore, the defined catchment boundaries allow for an assessment of the reported uncertainties within each catchment.
344 If needed the catchment boundaries delivered with CAMELS-DE can be used to calculate the reported uncertainties of
345 SoilGrids within each catchment.

346 **5.5 Hydrogeology**

347 The hydrogeological attributes for CAMELS-DE are derived from the hydrogeological overview map of Germany on the
348 scale of 1:250,000; "HÜK250" (HGM250, 2019), which describes the hydrogeological characteristics of the upper,
349 large-scale contiguous aquifers in Germany. For CAMELS-DE, the areal percentage of the various HÜK250 classes (see
350 Tab. 2) was calculated for each catchment, whereby the variables of the classes permeability, aquifer media type, cavity type,
351 consolidation, rock type and geochemical rock type sum to 100 percent. Uncertainties in these data may arise from the

352 generalisation required to scale point measurements to a gridded product, which can oversimplify complex hydrogeological
353 features, potentially leading to inaccuracies in the representation of local variations and the spatial distribution of aquifer
354 properties.

355 **5.6 Human influence**

356 CAMELS-DE includes information on human influences within catchments, primarily focusing on existing dams and
357 reservoirs in Germany. This information is sourced from the inventory of dams in Germany (Speckhann et al., 2021), which
358 offers detailed data including dam names, locations, associated rivers, years of construction and operation start, crest lengths,
359 dam heights, lake areas, lake volumes, purposes (such as flood control or water supply), dam structure types, and specific
360 building characteristics for 530 dams across Germany. For catchments containing multiple dams, this data is aggregated to
361 provide a comprehensive overview. Specifically, CAMELS-DE includes key information about the dams within each
362 catchment, such as the number of dams, the names of the dams, the rivers where these dams are located, the operational
363 years of the oldest and newest dams, the total area and volume of all dam lakes at full capacity, and the overall purposes of
364 these dams. It is important to note that the “Inventory of Dams in Germany” does not claim to be exhaustive. The absence of
365 recorded dams in this inventory does not necessarily indicate a lack of human influence within a catchment. Nearly all
366 catchments in Germany experience substantial anthropogenic influences, and it is likely that some dams, weirs, or reservoirs
367 (particularly smaller ones) are not documented in the dataset. Another relevant indicator of human influence included in
368 CAMELS-DE is hence the proportion of artificial and agricultural surfaces derived from land cover attributes (see section
369 5.3).

370 **6 Benchmark LSTM and HBV model**

371 CAMELS-DE, in addition to hydro-meteorological observations and catchment attributes, includes results from data-driven
372 and conceptual lumped rainfall-runoff simulations for each catchment. More specifically, these results are derived from a
373 regionally trained LSTM network (trained on all catchments at the same time) and a locally trained lumped HBV model
374 (trained at each individual catchment; Bergström and Forsman, 1973, Seibert, 2005, Feng et al., 2022). These models serve
375 three main purposes: (a) they are used to identify catchments where the relationship between meteorological forcing and
376 streamflow is difficult to capture (low model performance), indicating possible strong human influences such as dams or
377 reservoirs, or potential issues with the catchment delineation or the streamflow or meteorological time series; (b) they can
378 serve as a benchmark for future modelling studies based on CAMELS-DE in a sense that the reported performance values
379 and time series can be used as a baseline model and (c) in case of a good model performance can be used to fill missing
380 values of the observed discharge time series. Both models were trained over the period from October 1, 1970, to December
381 31, 1999, validated from October 1, 1965, to September 30, 1970, and tested from January 1, 2000, to December 31, 2020.
382 CAMELS-DE includes the simulated discharges for both models for the entire 70 years (Tab. 1), a flag was added to indicate

383 if the corresponding time step was used in training, validation or testing. In the following we explain the model setups and
384 analyse the simulation results in detail. The code of the LSTM model and the HBV model were carefully tested and
385 benchmarked (Acuña Espinoza et al., 2024). The codes have been designed to allow easy access and a permalink to the code
386 version used for CAMELS-DE can be found here (<https://github.com/KIT-HYD/Hy2DL/tree/v1.1>, last access: 24 July 2024).

387 6.1 Setup LSTM model

388 The LSTM uses mean precipitation, standard deviation of precipitation, mean radiation, mean minimum temperature and
389 mean maximum temperature as dynamic (time varying) input features and specific discharge as a target variable. Static
390 features and hyperparameters were set according to the study of Acuña et al. (2024) with modifications made to (1) an
391 increased hidden size from 64 to 128 and (2) a reduced number of epochs from 30 to 20. The remaining hyperparameters
392 were set as follows: number of hidden layers = 1; learning rate = 0.001; dropout rate = 0.4; batch size = 256; sequence length
393 = 365 days; iterative optimization algorithm = Adam. We use the basin-averaged Nash-Sutcliffe Efficiency (NSE*) loss
394 function proposed by Kratzert et al. (2019) to avoid an imbalance during training due to the higher influence of catchments
395 with a higher runoff generation. In addition, to the model results (see Tab. 2), we provide the model training epochs of the
396 regional LSTM as part of the CAMELS-DE dataset.

397 6.2 Setup HBV model

398 The lumped HBV model used in CAMELS-DE is a variant of the well-known HBV (Hydrologiska Byråns
399 Vattenbalansavdelning; Bergström and Forsman, 1973) model. A detailed description of the model architecture and setup can
400 be found in the studies by Seibert (2005) and Feng et al. (2022). HBV uses mean precipitation and potential
401 evapotranspiration (E_{pot} ; mm d^{-1}) as inputs. The E_{pot} is calculated using the temperature-based Hargreaves formula, detailed
402 by Adam et al. (2006) and based on earlier work by Droogers and Allen (2002), as explained and cited in
403 Clerc-Schwarzenbach et al. (2024). This variant of the Hargreaves formula resulted in the lowest mass balance error in most
404 catchments with respect to other methods (e.g. Penman, Priestly Taylor) to estimate evapotranspiration and was additionally
405 chosen due to its low data requirements, enabling the utilisation of HYRAS precipitation and temperature data to generate
406 the E_{pot} time series with a limited number of assumptions. The E_{pot} time series are included in CAMELS-DE (Tab. 2) for the
407 entire time period of 70 years. In terms of model calibration, the SHM was trained individually for each basin using the NSE
408 as a loss function, employing the Differential Evolution Adaptive Metropolis (DREAM; Vrugt, 2016) algorithm as
409 implemented in the SPOTPY (SPOTting model parameters using a ready-made PYthon package, Houska et al., 2015)
410 library. In contrast to the LSTM, the SHM model is mass conserving and hence more sensitive to errors in the catchment
411 delineation that can lead to mass balance errors (see section 3). The difference between the SHM and the LSTM performance
412 can be seen as an indicator either for a strong human influence or for an imprecise catchment delineation as the LSTM can
413 create mass. In addition to the model results (see Tab. 2), we provide the HBV model parameters for each catchment as part
414 of the CAMELS-DE dataset.

415 6.3 Results LSTM and SHM model

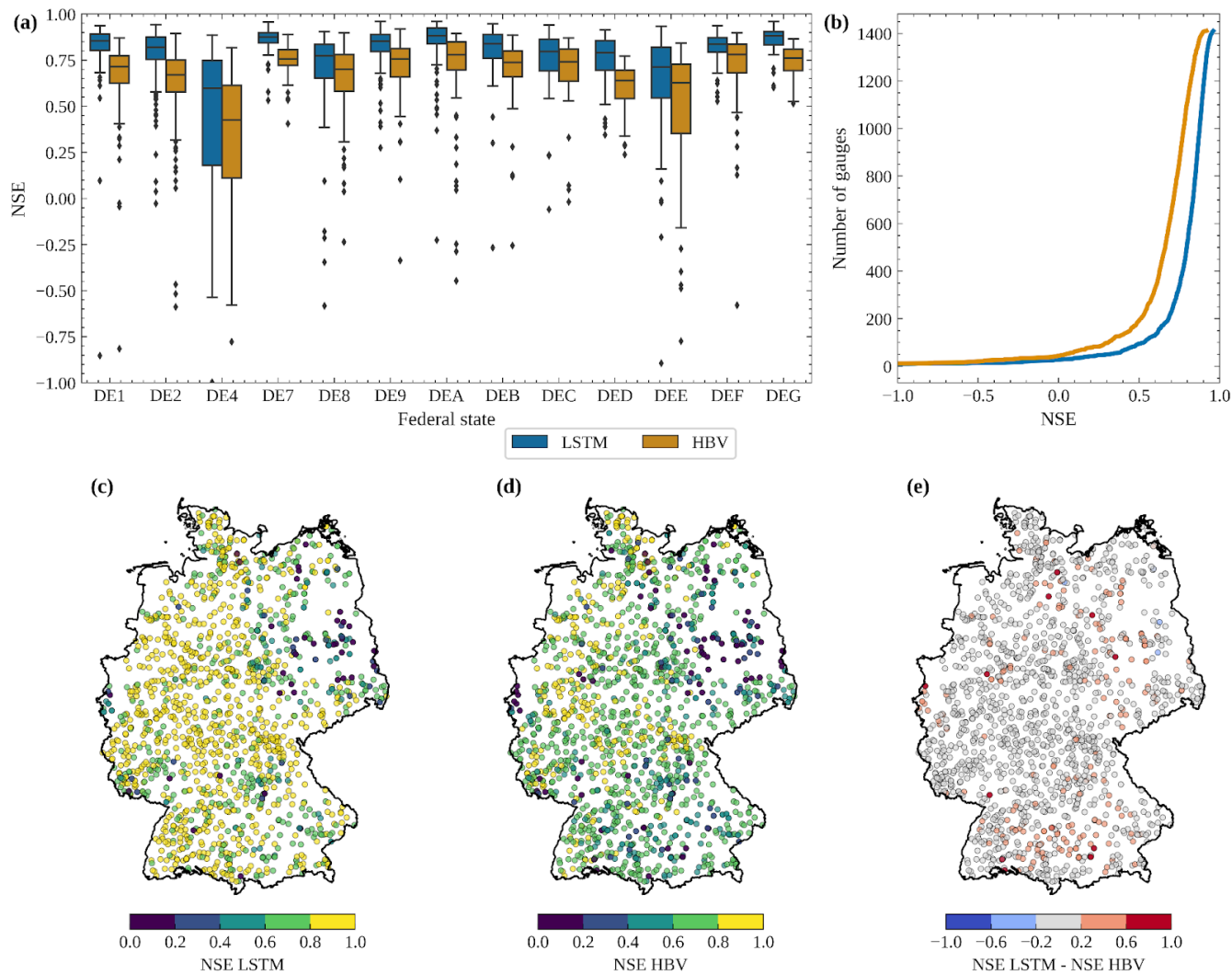
416 In this section, we focus our analysis on the LSTM and SHM model in catchments where at least 20 % of the daily data is
417 available during the 30-year training period and 10 % during the testing period, covering a total of 1411 catchments. The
418 median performance of the LSTM, as quantified by the NSE during the testing period, is 0.84 across 1411 catchments. Of
419 these, 94 catchments have an NSE lower than 0.5 (6.66 % of all catchments), out of which 28 have a negative NSE (1.98 %
420 of all catchments). For the 94 catchments with NSE below 0.5, most streamflow time series exhibit a low Pearson correlation
421 with daily precipitation (< 0.1) and these catchments are often considerably affected by the construction and/or operation of
422 dams or flood control structures (human influences attributes). Therefore, model performance of the LSTM network can be
423 used to identify catchments that are subject to considerable uncertainties, either due to measurement inaccuracies or
424 significant human influences.

425

426 Fig. 5a illustrates the performance of the LSTM model across various federal states, with relatively consistent results across
427 the board except for the federal states of Brandenburg (DE4) and Saxony-Anhalt (DEE). In Brandenburg, lowland
428 catchments characterised by sandy soils, considerable groundwater impacts, abundance of natural lakes and human
429 constructed weirs, canals and cross-connections between streams most likely yield a distinctly lower model performance
430 compared to the rest of the German federal states. Besides the federal state of Brandenburg and Saxony-Anhalt the analysis
431 of the LSTMs simulations reveals no clear correlation between the model performance and the topographic attributes (e.g.,
432 area), climatic attributes (e.g., long-term mean precipitation), or hydrological attributes (e.g., long-term mean flow).

433

434 The performance of HBV is with a median NSE of 0.72 lower than that of the LSTM (Fig. 5b). In 192 catchments (13.61 %)
435 the HBV shows a performance below a NSE of 0.5 and in 44 (3.12 %) a performance below a NSE of 0. The spatial patterns
436 of performance measured by the NSE are consistent between the LSTM and HBV. In other words, catchments where the
437 LSTM performs well are typically also accurately represented by HBV, and vice versa, as illustrated in Fig. 5e. Catchments
438 in which HBV significantly underperforms compared to the LSTM are almost invariably strongly influenced by
439 human-made structures such as dams or weirs, or they are located in areas with uncertain catchment delineation. We propose
440 that the HBV model, which conserves mass and uses time-invariant parameters, struggles to adapt to dynamic changes in
441 catchment function caused by human activities that result in inaccuracies in water flow and storage due to structures like
442 dams, weirs or due to irrigation or pumping. A hypothesis that requires further testing in the few catchments where this is the
443 case.



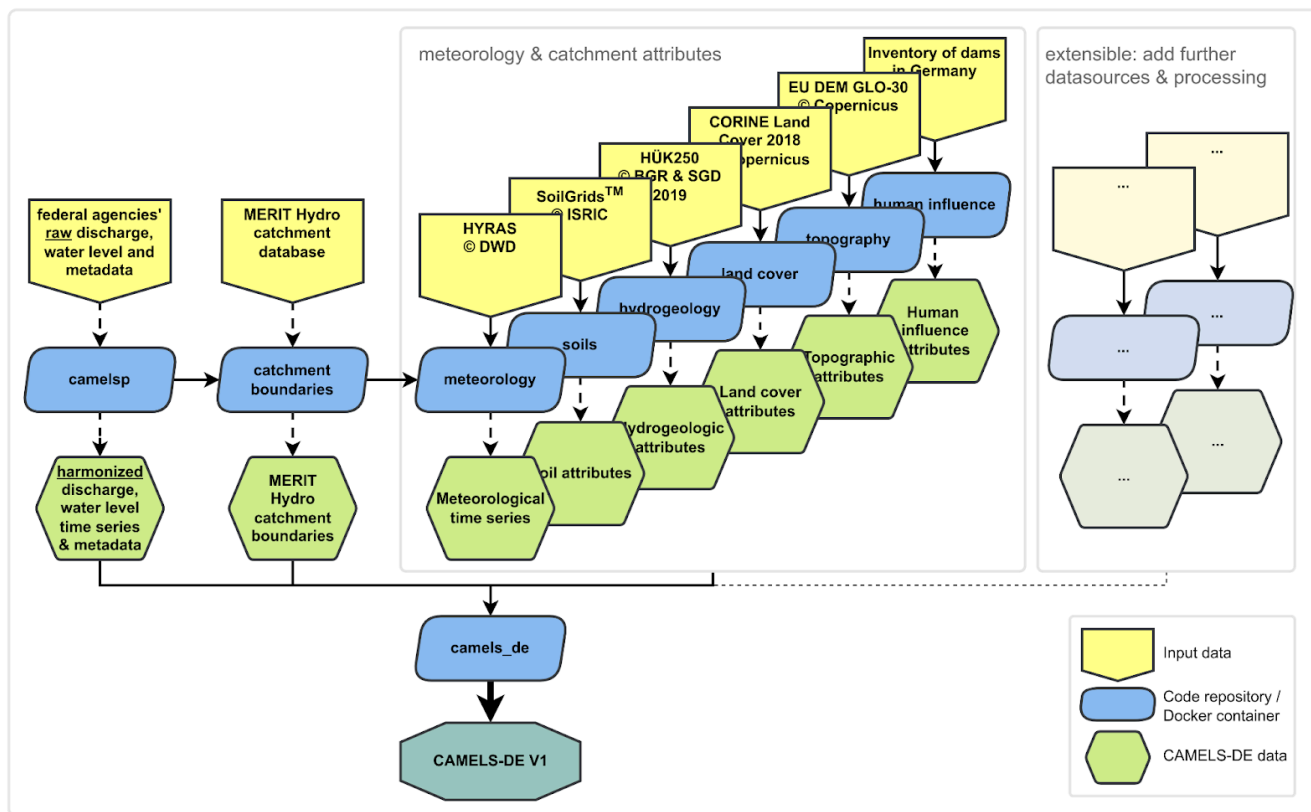
444

445 **Figure 5:** Panel (a) shows boxplots visualising the distribution of the NSE of the LSTM network (blue) and the HBV model (orange) for each federal state
 446 in Germany for the testing period. Panel (b) shows a cumulative plot of the NSE for the general comparison of the LSTM model and the HBV model. Panel
 447 (c) shows the NSE values of the LSTM for 1411 gauging stations in Germany, while panel (c) shows the same for the NSE values of the HBV model. Panel
 448 (e) shows the difference between the NSE values of the LSTM and the HBV model for all gauging stations in Germany, borders of Germany: ©
 449 GeoBasis-DE / BKG (VG250, 2023)

450 7 Code availability, reproducibility and extensions

451 The processing of CAMELS-DE is structured in a modular manner to enhance the clarity and reproducibility of the
 452 processing pipeline. The CAMELS-DE processing pipeline was published separately with more details and permalinks to the
 453 released repository versions that represent the code state that was used to process and compile CAMELS-DE (Dolich, 2024).

454 For each component of CAMELS-DE, a distinct GitHub repository was established. Within each repository, a dedicated
455 Docker container was developed to process specific input datasets (e.g. HYRAS, GLO-30 DEM). Containerization is
456 particularly well-suited for this project as it ensures that each component of the data processing pipeline runs consistently
457 across different computing environments. This containerization simplifies dependency management, enhances
458 reproducibility, and facilitates the deployment and version control of each processing module. Fig. 6 illustrates the
459 architecture of the processing pipeline, where each blue block represents an individual GitHub repository equipped with a
460 Docker container that processes the yellow input data to produce the green output data. All repositories are uniformly
461 structured, and the accompanying documentation provides detailed descriptions of each repository, guidelines for building
462 and running the Docker containers, including the necessary folder mounts, and instructions for accessing the required input
463 data. In the initial phase of the CAMELS-DE data processing pipeline, raw discharge and water level data, along with station
464 metadata provided by the federal states, are processed and harmonised. Subsequently, MERIT-Hydro catchment boundaries
465 are delineated for each station, a pivotal step since all further datasets depend extensively on these catchment boundaries.
466 Meteorological time series data for these catchments are then processed to compute statistics such as area mean and median.
467 Following this, attributes such as soil properties, hydrogeology, land cover, topography, and human influences are derived for
468 each catchment (see Table 2). In the final stage, all derived data are integrated and formatted according to the established
469 structure of the CAMELS-DE dataset, mirroring the organisational schema of CAMELS-GB or CAMELS-CH.



470

471 **Figure 6:** Diagram of the CAMELS-DE data processing pipeline. Starting with raw discharge and metadata harmonisation, it proceeds to derive
 472 MERIT-Hydro catchment boundaries. Subsequent processing includes meteorological data extraction and aggregation followed by the extraction of various
 473 catchment attributes. In the final step, all extracted data sources are integrated in the structured CAMELS-DE dataset, consistent with CAMELS-GB or
 474 CAMELS-CH (Dolich, 2024).

475 The modular design of the CAMELS-DE processing pipeline enhances its traceability, comprehensibility, and
 476 reproducibility, differing significantly from a monolithic code approach that compiles the entire dataset into a single
 477 repository. This structure not only facilitates the extension of the pipeline to incorporate additional data sources, especially
 478 further catchment attributes, without the need to re-run or rewrite the entire system but also allows for the adaptation of
 479 processing or aggregation methods and the seamless release of updated versions of the CAMELS-DE dataset. The publicly
 480 available Docker containers and the code within them serve not only as a comprehensive guide to understanding the data
 481 processing methods used in CAMELS-DE but also provide a foundation for further data processing using the catchment
 482 geometries included in the dataset. We encourage researchers to enrich CAMELS-DE with additional data sources and
 483 explore ways to enhance the baseline model results. Such contributions are invaluable for continuous improvements and
 484 expansions of the CAMELS-DE dataset, reflecting our commitment to advancing hydrological research and applications
 485 through reproducible science.

486 8 Data availability

487 This manuscript describes the state of version 1.0 of CAMELS-DE, which is freely available at
488 <https://doi.org/10.5281/zenodo.13837553> (Dolich et al., 2024), accompanied by a comprehensive data description. The code
489 to reproduce CAMELS-DE can be found at <https://doi.org/10.5281/zenodo.12760336> (Dolich, 2024).

490 9 Conclusions

491 CAMELS-DE is a significant step forward in hydrological research for Germany and beyond, offering a comprehensive
492 dataset that spans 1582 catchments with hydro-meteorological daily time series from 1951 to 2020. CAMELS-DE includes
493 detailed catchment delineations and properties, such as reservoir data, land-use, soils, and hydrogeology, which are all vital
494 to analyse and describe the local and regional hydrology of Germany. Furthermore, CAMELS-DE includes simulations from
495 a regionally trained LSTM and locally trained HBV model that can be used either to fill gaps in discharge data in case of
496 good model performance or act as baseline models for the development and testing of new hydrological models. Due to the
497 length of the provided time series of up to 70 years CAMELS-DE opens up new opportunities for investigating long-term
498 hydrological trends or conducting large-sample studies across diverse catchments, including a large number of catchments
499 smaller than 100 km². The dataset's modular design, achieved through the containerization of each processing component,
500 ensures that the data processing is traceable, comprehensible, and reproducible. This approach makes it easier to extend the
501 dataset by incorporating new data sources, adapting processing methods, and releasing updated versions without the need to
502 re-run the entire pipeline. While CAMELS-DE serves as a useful benchmark for large sample hydrology, we invite the
503 scientific community to enrich it with additional data sources and improved methods. In conclusion, CAMELS-DE aims to
504 support a broad range of hydrological research and applications, to foster better understanding and management of water
505 resources in Germany and beyond and to contribute to future global hydrological studies.

506

507 **Author contribution:** RL and MS initiated the CAMELS-DE project. AD prepared and processed data, created most figures
508 and wrote together with RL most of the manuscript. All other authors suggested improvements and made additions to the
509 manuscript, as well as provided data and expertise for specific topics.

510

511 **Competing interests:** At least one of the (co-)authors is a member of the editorial board of Earth System Science Data or
512 Hydrology and Earth System Sciences.

513

514 **Acknowledgment:** We thank the various German institutions for providing observation-based data and sharing their
515 expertise. We are grateful to the Volkswagen Foundation for funding the “CAMELS-DE” project within the framework of

516 the project "Invigorating Hydrological Science and Teaching: Merging Key Legacies with New Concepts and Paradigms"
 517 (ViTamins). We also extend our thanks to NFDI4Earth, particularly Jörg Seegert, for their support and suggestions.
 518

519 **Table 2.:** Catchment-specific static attributes available in CAMELS-DE

Attribute class	Attribute name	Description	Unit	Data source
Location and topography	gauge_id	catchment identifier based on the NUTS classification as described in section 5.1 e.g. DE110000, DE110010, ...	–	Federal state agencies (see section 2)
	provider_id	official gauging station ID assigned by the federal states	–	
	gauge_name	gauging station name		
	water_body_name	water body name	–	
	federal_state	federal state in which the measuring station is located		
	gauge_lon	gauging station longitude (EPSG:4326)	°	
	gauge_lat	gauging station latitude (EPSG:4326)	°	
	gauge_easting	gauging station easting (EPSG:3035)	m	
	gauge_northing	gauging station northing (EPSG:3035)	m	
	gauge_elev_metadata	gauging station elevation as given by the federal states	m a.s.l.	
area_metadata	catchment area as given by the federal states	km ²		
	gauge_elev	gauging station elevation derived from the GLO-30 DEM	m a.s.l.	Copernicus GLO-30 DEM (EU-DEM, 2022)
	area	catchment area derived from the MERIT Hydro catchment	km ²	
	elev_mean	mean elevation in the catchment based on the MERIT Hydro geometry	m a.s.l.	
	elev_min	minimum elevation within catchment	m a.s.l.	
	elev_5	5th percentile elevation within catchment	m a.s.l.	
	elev_50	median elevation within catchment	m a.s.l.	
	elev_95	95th percentile elevation within catchment	m a.s.l.	

	elev_max	maximum elevation within catchment	m a.s.l.	
Climate	p_mean	long-term mean of daily precipitation from 1951 to 2020	mm d ⁻¹	German Weather Service HYRAS (DWD-HYRAS, 2024)
	p_seasonality	seasonality and timing of precipitation (estimated using sine curves to represent the annual temperature and precipitation cycles, positive (negative) values indicate that precipitation peaks in summer (winter), and values close to zero indicate uniform precipitation throughout the year).	–	
	frac_snow	fraction of precipitation falling as snow, i.e. while mean air temperature is < 0° C	–	
	high_prec_freq	frequency of high-precipitation days (≥ 5 times mean daily precipitation)	d yr ⁻¹	
	high_prec_dur	mean duration of high-precipitation events (number of consecutive days ≥ 5 times mean daily precipitation)	d	
	high_prec_timing	season during which most high-precipitation days occur, e.g. 'jja' for summer. If two seasons register the same number of events a value of NA is given.	season	
	low_prec_freq	frequency of dry days (< 1 mm d ⁻¹)	d yr ⁻¹	
	low_prec_dur	mean duration of dry periods (number of consecutive days < 1 mm d ⁻¹ mean daily precipitation)	d	
	low_prec_timing	season during which most dry season days occur, e.g. 'son' for autumn. If two seasons register the same number of events a value of NA is given.	season	
Hydrology	q_mean	mean daily specific discharge	mm d ⁻¹	Federal state agencies (see section 3.1) and German Weather Service HYRAS (DWD-HYRAS, 2024)
	runoff_ratio	runoff ratio (ratio of mean daily discharge to mean daily precipitation)	–	
	flow_period_start	first date for which daily streamflow data is available	–	
	flow_period_end	last day for which daily streamflow data is available	–	
	flow_perc_complete	percentage of days for which streamflow data is available from Jan 1951–31 Dec 2020	%	
	slope_fdc	slope of the flow duration curve (between the log-transformed 33rd and 66th stream flow percentiles, see Coxon et al. (2020))	–	
	hfd_mean	mean half-flow date (number of days since 1.	d	

		Oct at which the cumulative dis charge reaches half of the annual discharge)		
	Q5	5 % flow quantile (low flow)	mm d ⁻¹	
	Q95	95 % flow quantile (high flow)	mm d ⁻¹	
	high_q_freq	frequency of high-flow days (> 9 times the median daily flow)	d yr ⁻¹	
	high_q_dur	mean duration of high-flow events (number of consecutive days > 9 times the median daily flow)	d	
	low_q_freq	frequency of low-flow days (< 0.2 times the mean daily flow)	d yr ⁻¹	
	low_q_dur	mean duration of low-flow events (number of consecutive days < 0.2 times the mean daily flow)	d	
	zero_q_freq	fraction of days with zero stream flow	–	
Land cover	artificial_surfaces_perc	areal coverage of artificial surfaces	%	CORINE Land Cover 2018 (CLC, 2018)
	agricultural_areas_perc	areal coverage of agricultural areas	%	
	forests_and_seminatural_areas_perc	areal coverage of forests and semi-natural areas	%	
	wetlands_perc	areal coverage of wetlands	%	
	water_bodies_perc	areal coverage of water bodies	%	
Soil	clay_0_30cm_mean clay_30_100cm_mean clay_100_200cm_mean	weight percent of clay particles (< 0.002 mm) in the fine earth fraction at depths 0 - 30 cm, 30 - 100 cm and 100 - 200 cm	wt. %	SoilGrids250m (Poggio et al., 2021)
	silt_0_30cm_mean silt_30_100cm_mean silt_100_200cm_mean	weight percent of silt particles (≥ 0.002 mm and ≤ 0.05/0.063 mm) in the fine earth fraction at depths 0 - 30 cm, 30 - 100 cm and 100 - 200 cm	wt. %	
	sand_0_30cm_mean sand_30_100cm_mean sand_100_200cm_mean	weight percent of sand particles (> 0.05/0.063 mm) at depths 0 - 30 cm, 30 - 100 cm and 100 - 200 cm	wt. %	
	coarse_fragments_0_30cm_mean coarse_fragments_30_100cm_mean coarse_fragments_100_200cm_mean	volumetric fraction of coarse fragments (> 2 mm) at depths 0 - 30 cm, 30 - 100 cm and 100 - 200 cm	vol %	
	soil_organic_carbon_0_30cm_mean soil_organic_carbon_30_100cm_mean soil_organic_carbon_100_200cm_mean	soil organic carbon content in the fine earth fraction at depths 0 - 30 cm, 30 - 100 cm and 100 - 200 cm	g kg ⁻¹	

	bulk_density_0_30cm_mean bulk_density_30_100cm_mean bulk_density_100_200cm_mean	bulk density of the fine earth fraction at depths 0 - 30 cm, 30 - 100 cm and 100 - 200 cm	kg dm ⁻³	
Hydrogeology	aquitard_perc aquifer_perc aquifer_aquitard_mixed_perc	areal coverage of aquifer media type classes	%	HÜK250 © BGR & SGD (Staatlichen Geologischen Dienste) 2019 (HGM, 2019)
	kf_very_high_perc (>1E-2 m s ⁻¹) kf_high_perc (>1E-3 – 1E-2 m s ⁻¹) kf_medium_perc (>1E-4 – 1E-3 m s ⁻¹) kf_moderate_perc ((>1E-5 – 1E-4 m s ⁻¹) kf_low_perc (>1E-7 – 1E-5 m s ⁻¹) kf_very_low_perc (>1E-9 - 1E-7 m s ⁻¹) kf_extremely_low_perc (<1E-9 m s ⁻¹) kf_very_high_to_high_perc (>1E-3 m s ⁻¹) kf_medium_to_moderate_perc (>1E-5 – 1E-3 m s ⁻¹) kf_low_to_extremely_low_perc (<1E-5 m s ⁻¹) kf_highly_variable_perc kf_moderate_to_low_perc (>1E-6 – 1E-4 m s ⁻¹)	areal coverage of permeability classes	%	
	cavity_fissure_perc cavity_pores_perc cavity_fissure_karst_perc cavity_fissure_pores_perc	areal coverage of cavity type classes	%	
	consolidation_solid_rock_perc consolidation_unconsolidated_rock_perc	areal coverage of consolidation classes	%	
	rocktype_sediment_perc rocktype_metamorphite_perc rocktype_magmatite_perc	areal coverage of rock type classes	%	
	geochemical_rocktype_silicate_perc geochemical_rocktype_silicate_carbonatic_perc geochemical_rocktype_carbonatic_perc geochemical_rocktype_sulfatic_perc geochemical_rocktype_silicate_organic_components_perc geochemical_rocktype_anthropogenically_modified_through_filling_perc geochemical_rocktype_sulfatic_halitic_perc geochemical_rocktype_halitic_perc	areal coverage of geochemical rock type classes	%	

c

	waterbody_perc	areal coverage of water body areas according to hydrogeological map	%	
	no_data_perc	percentage of areas with missing data	%	
Human influence	dams_names	names of all dams located in the catchment	–	Inventory of dams in Germany (Speckhann et al., 2021)
	dams_river_names	names of the rivers where the dams are located	–	
	dams_num	number of dams located in the catchment	–	
	dams_year_first	year when the first dam entered operation	–	
	dams_year_last	year when the last dam entered operation	–	
	dams_total_lake_area	total area of all dam lakes at full capacity	km ²	
	dams_total_lake_volume	total volume of all dam lakes at full capacity	Mio m ³	
	dams_purposes	purposes of all the dams in the catchment	–	
Hydrological Simulations	training_perc_complete	percentage of observed specific discharge values in the training period (1970-10-01 – 1999-12-31) that are not NaN	%	Regional LSTM model, HBV model (see section 6, https://github.com/KIT-HYD/Hy2DL/tree/v1.1 , last access: 24 July 2024)
	validation_perc_complete	percentage of observed specific discharge values in the validation period (1965-10-01 – 1970-09-30) that are not NaN	%	
	testing_perc_complete	percentage of observed specific discharge values in the testing period (2001-10-01 – 2020-12-31) that are not NaN	%	
	NSE_lstm	Nash-Sutcliffe model efficiency coefficient of the LSTM in the testing period	–	
	NSE_hbv	Nash-Sutcliffe model efficiency coefficient of the HBV model in the testing period	–	

520

521 References

522 Acuña Espinoza, E., Loritz, R., Álvarez Chaves, M., Bäuerle, N., and Ehret, U.: To bucket or not to bucket? Analyzing the
 523 performance and interpretability of hybrid hydrological models with dynamic parameterization, *Hydrology and Earth
 524 System Sciences*, 28, 2705–2719, <https://doi.org/10.5194/hess-28-2705-2024>, 2024.

525 Adam, J. C., Clark, E. A., Lettenmaier, D. P., and Wood, E. F.: Correction of global precipitation products for orographic
 526 effects, *J. Clim.*, 19, 15–38, <https://doi.org/10.1175/JCLI3604.1>, 2006.

527 Addor, N., Newman, A. J., Mizukami, N., and Clark, M. P.: The CAMELS data set: catchment attributes and meteorology
528 for large-sample studies, *Hydrology and Earth System Sciences*, 21, 5293–5313, <https://doi.org/10.5194/hess-21-5293-2017>,
529 2017.

530 Bergström, S. and Forsman, A.: Development of a Conceptual Deterministic Rainfall-runoff Model, *Hydrology Research*, 4,
531 147–170, <https://doi.org/10.2166/nh.1973.0012>, 1973.

532 Brunner, M. I., Slater, L., Tallaksen, L. M., and Clark, M.: Challenges in modeling and predicting floods and droughts: A
533 review, *WIREs Water*, 8, <https://doi.org/10.1002/wat2.1520>, 2021.

534 CLC: Corine Land Cover <https://doi.org/10.2909/960998c1-1870-4e82-8051-6485205ebbac> (last access: 24 July 2024),
535 2018.

536 Clerc-Schwarzenbach, F. M., Selleri, G., Neri, M., Toth, E., van Meerveld, I., and Seibert, J.: HESS Opinions: A few camels
537 or a whole caravan?, *EGUsphere* [preprint], <https://doi.org/10.5194/egusphere-2024-864>, 2024.

538 Coxon, G., Addor, N., Bloomfield, J. P., Freer, J., Fry, M., Hannaford, J., Howden, N. J. K., Lane, R., Lewis, M., Robinson,
539 E. L., Wagener, T., and Woods, R.: CAMELS-GB: hydrometeorological time series and landscape attributes for 671
540 catchments in Great Britain, *Earth System Science Data*, 12, 2459–2483, <https://doi.org/10.5194/essd-12-2459-2020>, 2020.

541 Dolich, A., Espinoza, E. A., Ebeling, P., Guse, B., Götte, J., Hassler, S., Hauffe, C., Kiesel, J., Heidbüchel, I., Mälicke, M.,
542 Müller-Thomy, H., Stölzle, M., Tarasova, L., & Loritz, R.: CAMELS-DE: hydrometeorological time series and attributes for
543 1582 catchments in Germany (1.0.0) [Data set]. Zenodo. <https://doi.org/10.5281/zenodo.13837553>, 2024

544 Dolich, A.: CAMELS-DE Processing Pipeline, Zenodo, <https://doi.org/10.5281/zenodo.13842287>, 2024

545 Droogers, P. and Allen, R. G.: Estimating reference evapotranspiration under inaccurate data conditions, *Irrig. Drain. Syst.*,
546 16, 33–45, <https://doi.org/10.1023/A:1015508322413>, 2002.

547 DWD-HYRAS: <https://www.dwd.de/DE/leistungen/hyras/hyras.html> (last access: 25 March 2024), 2024.

548 Ebeling, P., Kumar, R., Lutz, S. R., Nguyen, T., Sarrazin, F., Weber, M., Büttner, O., Attinger, S., and Musolff, A.:
549 QUADICA: water QUALity, DIScharge and Catchment Attributes for large-sample studies in Germany, *Earth System Science*
550 *Data*, 14, 3715–3741, <https://doi.org/10.5194/essd-14-3715-2022>, 2022.

551 Eiselt, K.-U., Kaspar, F., Mölg, T., Krähenmann, S., Posada, R., and Riede, J. O.: Evaluation of gridding procedures for air
552 temperature over Southern Africa, *Advances in Science and Research*, 14, 163–173,
553 <https://doi.org/10.5194/asr-14-163-2017>, 2017.

554 EU-DEM: Copernicus GLO-30 DEM, <https://doi.org/10.5270/esa-c5d3d65> (last access: 24 July 2024), 2022.

555 Färber, C., Plessow, H., Kratzert, F., Addor, N., Shalev, G., & Looser, U.: GRDC-Caravan: extending the original dataset
556 with data from the Global Runoff Data Centre (0.2) [Data set]. Zenodo. <https://doi.org/10.5281/zenodo.10074416>, 2023.

557 Feng, D., Liu, J., Lawson, K., & Shen, C.: Differentiable, learnable, regionalized process-based models with multiphysical
558 outputs can approach state-of-the-art hydrologic prediction accuracy. *Water Resources Research*, 58, e2022WR032404.
559 <https://doi.org/10.1029/2022WR032404>, 2022.

560 Heberger, M.: delineator.py: Fast, accurate watershed delineation using hybrid vector- and raster-based methods and data
561 from MERIT-Hydro (v1.3). Zenodo. <https://doi.org/10.5281/zenodo.10143149>, 2023.

562 HGM250: Hydrogeological Map of Germany (1:250,000), [https://gdk.gdi-de.org/geonetwork/srv/api/records/
563 61ac4628-6b62-48c6-89b8-46270819f0d6](https://gdk.gdi-de.org/geonetwork/srv/api/records/61ac4628-6b62-48c6-89b8-46270819f0d6) (last access: 24 July 2024), 2019.

564 Hochreiter, S., & Schmidhuber, J.: Long short-term memory. *Neural Computation*, 9(8), 1735–1780.
565 <https://doi.org/10.1162/neco.1997.9.8.1735>, 1997.

566 Hochreiter, S.: The vanishing gradient problem during learning recurrent neural nets and problem solutions. *International
567 Journal of Uncertainty, Fuzziness and Knowledge-Based Systems*, 06(02), 107–116.
568 <https://doi.org/10.1142/s0218488598000094>, 1998.

569 Houska, T., Kraft, P., Chamorro-Chavez, A., and Breuer, L.: SPOTting Model Parameters Using a Ready-Made Python
570 Package, *PLOS ONE*, 10, e0145180, <https://doi.org/10.1371/journal.pone.0145180>, 2015.

571 Höge, M., Kauzlaric, M., Siber, R., Schönenberger, U., Horton, P., Schwanbeck, J., Floriancic, M. G., Viviroli, D., Wilhelm,
572 S., Sikorska-Senoner, A. E., Addor, N., Brunner, M., Pool, S., Zappa, M., and Fenicia, F.: CAMELS-CH:
573 hydro-meteorological time series and landscape attributes for 331 catchments in hydrologic Switzerland, *Earth System
574 Science Data*, 15, 5755–5784, <https://doi.org/10.5194/essd-15-5755-2023>, 2023.

575 HYRAS-DE-HURS: Raster data set of daily mean relative humidity in % for Germany - HYRAS-DE-HURS, Version v5.0,
576 [https://opendata.dwd.de/climate_environment/CDC/grids_germany/multi_annual/hyras_de/humidity/DESCRIPTION_GRD_
577 DEU_P30Y_RH_HYRAS_DE_en.pdf](https://opendata.dwd.de/climate_environment/CDC/grids_germany/multi_annual/hyras_de/humidity/DESCRIPTION_GRD_DEU_P30Y_RH_HYRAS_DE_en.pdf) (last access: 24 July 2024), 2022.

578 HYRAS-DE-PRE: Raster data set of daily sums of precipitation in mm for Germany - HYRAS-DE-PRE, Version v5.0,
579 [https://opendata.dwd.de/climate_environment/CDC/grids_germany/daily/hyras_de/precipitation/DESCRIPTION_GRD_
580 U_PID_RR_HYRAS-DE_en.pdf](https://opendata.dwd.de/climate_environment/CDC/grids_germany/daily/hyras_de/precipitation/DESCRIPTION_GRD_DEU_PID_RR_HYRAS-DE_en.pdf) (last access: 24 July 2024), 2022.

581 HYRAS-DE-RSDS: Raster data set of daily mean global radiation in W/m² for Germany - HYRAS-DE-RSDS,
582 [https://opendata.dwd.de/climate_environment/CDC/grids_germany/daily/hyras_de/radiation_global/DESCRIPTION_GRD_](https://opendata.dwd.de/climate_environment/CDC/grids_germany/daily/hyras_de/radiation_global/DESCRIPTION_GRD_DEU_PID_RAD_G_HYRAS_DE_en.pdf)
583 [DEU_PID_RAD_G_HYRAS_DE_en.pdf](https://opendata.dwd.de/climate_environment/CDC/grids_germany/daily/hyras_de/radiation_global/DESCRIPTION_GRD_DEU_PID_RAD_G_HYRAS_DE_en.pdf) (last access: 24 July 2024), Version v3.0, 2023.

584 HYRAS-DE-TAS: Raster data set of daily mean temperature in °C for Germany - HYRAS-DE-TAS, Version v5.0,
585 [https://opendata.dwd.de/climate_environment/CDC/grids_germany/daily/hyras_de/air_temperature_mean/DESCRIPTION_](https://opendata.dwd.de/climate_environment/CDC/grids_germany/daily/hyras_de/air_temperature_mean/DESCRIPTION_GRD_DEU_PID_T2M_HYRAS_DE_en.pdf)
586 [GRD_DEU_PID_T2M_HYRAS_DE_en.pdf](https://opendata.dwd.de/climate_environment/CDC/grids_germany/daily/hyras_de/air_temperature_mean/DESCRIPTION_GRD_DEU_PID_T2M_HYRAS_DE_en.pdf) (last access: 24 July 2024), 2022.

587 HYRAS-DE-TASMAX: Raster data set of daily maximum temperature in °C for Germany - HYRAS-DE-TASMAX,
588 Version v5.0,
589 [https://opendata.dwd.de/climate_environment/CDC/grids_germany/monthly/hyras_de/air_temperature_max/DESCRIPTION_](https://opendata.dwd.de/climate_environment/CDC/grids_germany/monthly/hyras_de/air_temperature_max/DESCRIPTION_GRD_DEU_P1M_T2M_X_HYRAS_DE_en.pdf)
590 [GRD_DEU_P1M_T2M_X_HYRAS_DE_en.pdf](https://opendata.dwd.de/climate_environment/CDC/grids_germany/monthly/hyras_de/air_temperature_max/DESCRIPTION_GRD_DEU_P1M_T2M_X_HYRAS_DE_en.pdf) (last access: 24 July 2024), 2022.

591 HYRAS-DE-TASMIN: Raster data set of daily minimum temperature in °C for Germany - HYRAS-DE-TASMIN, Version
592 v5.0,
593 [https://opendata.dwd.de/climate_environment/CDC/grids_germany/daily/hyras_de/air_temperature_min/DESCRIPTION_G](https://opendata.dwd.de/climate_environment/CDC/grids_germany/daily/hyras_de/air_temperature_min/DESCRIPTION_RD_DEU_PID_T2M_N_HYRAS_DE_en.pdf)
594 [RD_DEU_PID_T2M_N_HYRAS_DE_en.pdf](https://opendata.dwd.de/climate_environment/CDC/grids_germany/daily/hyras_de/air_temperature_min/DESCRIPTION_RD_DEU_PID_T2M_N_HYRAS_DE_en.pdf) (last access: 24 July 2024), 2022.

595 Klingler, C., Schulz, K., and Herrnegger, M.: LamaH-CE: LARge-SaMple DATA for Hydrology and Environmental Sciences
596 for Central Europe, Earth System Science Data, 13, 4529–4565, <https://doi.org/10.5194/essd-13-4529-2021>, 2021.

597 Kratzert, F., Klotz, D., Shalev, G., Klambauer, G., Hochreiter, S., and Nearing, G.: Towards learning universal, regional, and
598 local hydrological behaviors via machine learning applied to large-sample datasets, Hydrology and Earth System Sciences,
599 23, 5089–5110, <https://doi.org/10.5194/hess-23-5089-2019>, 2019.

600 Lehner, B., Roth, A., Huber, M., Anand, M., Grill, G., Osterkamp, N., Tubbesing, R., Warmedinger, L., and Thieme, M.:
601 HydroSHEDS v2.0 – Refined global river network and catchment delineations from TanDEM-X elevation data, EGU
602 General Assembly 2021, online, 19–30 Apr 2021, EGU21-9277, <https://doi.org/10.5194/egusphere-egu21-9277>, 2021

603 Muñoz-Sabater, J., Dutra, E., Agustí-Panareda, A., Albergel, C., Arduini, G., Balsamo, G., Boussetta, S., Choulga, M.,
604 Harrigan, S., Hersbach, H., Martens, B., Miralles, D. G., Piles, M., Rodríguez-Fernández, N. J., Zsoter, E., Buontempo, C.,
605 and Thépaut, J.-N.: ERA5-Land: a state-of-the-art global reanalysis dataset for land applications, Earth System Science Data,
606 13, 4349–4383, <https://doi.org/10.5194/essd-13-4349-2021>, 2021.

607 Poggio, L., de Sousa, L. M., Batjes, N. H., Heuvelink, G. B. M., Kempen, B., Ribeiro, E., and Rossiter, D.: SoilGrids 2.0:
608 producing soil information for the globe with quantified spatial uncertainty, SOIL, 7, 217–240,
609 <https://doi.org/10.5194/soil-7-217-2021>, 2021.

610 Rauthe, M., Steiner, H., Riediger, U., Mazurkiewicz, A., and Gratzki, A.: A Central European precipitation climatology Part
611 I: Generation and validation of a high-resolution gridded daily data set (HYRAS), *Meteorologische Zeitschrift*, 22, 235–256,
612 <https://doi.org/10.1127/0941-2948/2013/0436>, 2013.

613 Razafimaharo, C., Krähenmann, S., Höpp, S., Rauthe, M., and Deutschländer, T.: New high-resolution gridded dataset of
614 daily mean, minimum, and maximum temperature and relative humidity for Central Europe (HYRAS), *Theoretical and
615 Applied Climatology*, 142, 1531–1553, <https://doi.org/10.1007/s00704-020-03388-w>, 2020.

616 Seibert, J., HBV Light Version 2. User’s Manual. Department of Physical Geography and Quaternary Geology, Stockholm
617 University, Stockholm, https://www.geo.uzh.ch/dam/jcr:c8afa73c-ac90-478e-a8c7-929eed7b1b62/HBV_manual_2005.pdf
618 (last access: 19. September 2024), 2005

619 Speckhann, G. A., Kreibich, H., and Merz, B.: Inventory of dams in Germany, *Earth System Science Data*, 13, 731–740,
620 <https://doi.org/10.5194/essd-13-731-2021>, 2021.

621 VG250: Verwaltungsgebiete 1:250 000 - Stand 01.01., [https://gdk.gdi-de.org/geonetwork/srv/api/records/
622 93a98c5c-cf03-4a95-bf0a-54001fbf3949](https://gdk.gdi-de.org/geonetwork/srv/api/records/93a98c5c-cf03-4a95-bf0a-54001fbf3949) (last access: 24 July 2024), 2023.

623 Vrugt, J. A.: Markov chain Monte Carlo simulation using the DREAM software package: Theory, concepts, and MATLAB
624 implementation, *Environmental Modelling & Software*, 75, 273–316, <https://doi.org/10.1016/j.envsoft.2015.08.013>,
625 2016.

626 Yamazaki, D., Ikeshima, D., Sosa, J., Bates, P. D., Allen, G. H., and Pavelsky, T. M.: MERIT Hydro: A High-Resolution
627 Global Hydrography Map Based on Latest Topography Dataset, *Water Resources Research*, 55, 5053–5073,
628 <https://doi.org/10.1029/2019wr024873>, 2019.

629 Yamazaki, D., Ikeshima, D., Tawatari, R., Yamaguchi, T., O’Loughlin, F., Neal, J. C., Sampson, C. C., Kanae, S., and Bates,
630 P. D.: A high-accuracy map of global terrain elevations, *Geophysical Research Letters*, 44, 5844–5853,
631 <https://doi.org/10.1002/2017gl072874>, 2017.